Removing darkness in images using the mobile application

S.E. Angel Anna Prathiba,
Assistant Professor,
Department of Computer Science and Engineering,
Erode Sengunthar Engineering College,
Perundurai, Erode, Tamilnadu, India.

S.Boopathirajan, V.Gunasekaran, K.Gowtham
Student
Department of Computer Science and Engineering,
Erode Sengunthar Engineering College,
Perundurai, Erode, Tamilnadu, India.

Abstract -The picture gives many feelings to all humans and it embedded to day today life everyone has mobile phones butwecan'ttakeclearphotosatnighttimetoovercomethisproblemusingthismobileapplication. Create a Mobile Application for Image Enhancement that help susercange to good image by using this mobile application. This also converts the dark image into a very clear image. This project used many image-processing python libraries for image enhancement. Also using python-KIVY to develop the mobile application. Using Bulldozer to convert the KIVY python file into the mobile application. 'Bulldozer' is a python-based tool that supports cross-platform and automates the build process for Android and also IOS applications. Onceuploadtheunclarityimageperformsoperationsandgivesagood-qualityimage. The mai n motive of the projects to improve the vintage image and unclear image in to a good image. It is very useful for low-quality camera mobiles.

Keywords: Image Enhancement; Image processing; Bulldozer; Python-based tool; Android Application.

I. INTRODUCTION

Due to in escapable environmental and/or technical limitations, many images are frequently taken in less-than-ideal lighting settings. They consist of in sufficient and imbalanced lighting in the environment, improper placement of it eosin front of strong backlight, and underexposure. When the picture was taken. Such that low-light images have poor visual quality and inadequate information transmission. While the latter results in an improper message being sent, such as in accurate object/face recognition, the former has an impact on the viewing experience.

1) To reduce the risk of over fitting, we present the first low light enhancement network that is independent of paired and unpaired training data. So, our approach generalizes effectively to a variety of lighting scenarios.
2) We create an image-specific line that, through the iterative application ,Maxville approximates both pixel-wised and higher-ordered curves. Such an image-specified curve can carry out mapping efficiently across a broad dynamic range.
3) Using a task-specified on-reference allows function that obliquely assesses the enhancement quality, we demonstrate the feasibility of training deep image to the enhancement model with out the reference photos.

II. RELATED WORK

1. Conventional methods. Traditional Techniques. HE-Based all techniques increase the dynamic range of a picture to highlight the light. Images' histogram distribution is altered at both the global [7, 10] and local [15, 27] levels. In addition, several techniques use the theory, which usually separates picture into reflectance and illumination. Light enhancement is framed as an illumination estimation problem because it is generally believed that the reflectancecomponentwillremainconstantregardlessofthelightingcircumstances. Multiple approaches have been put forth, all of which build the Retime hypothesis. Fu et al. suggested weighted variation model to concurrently assess the reflectance and illumination of an input picture; Wang et al. developed naturalness-and information-preserving technique when managing images of the non uniform illumination Goo et al. Li-et-lathe greatest intensity of each pixel in the RGB colour channels was scanned to estimate a crude

illumination map, which was then refined by all the structures before. This new Retime model will consider noise.

Through there solution of the power of the issue, the illumination map was equal to approximate. The suggested Zero DCE method generates an improved outcome through him-age specific curve mapping, in contrast to the usual methods that depend on possibly correct physical models or accidentally alter the distribution oft he image histogram. A method like this allows forpictureilluminationenhancementwithoutproducingartificialartifacts.Sun and Yuan. This project provides more stability, and a wider range of adjustment for the image dynamic range, and takes less computing work since it is data-driven and includes several light enhancement variables in the design of the non-reference loss functions.

2. Data-driven methods.

The two main divisions of the data-driven technique are CNN-based and GAN-based techniques. Many of CNN - based approaches require matched data for guided training, making the resource-intensive. The pair data are typically extensively obtained utilizing automated light degradation, modifying the camera settings while data is being recorded, or the data synthesis using picture retouching. For instance, the LL-Net was trained using information from a random gamma correction simulation

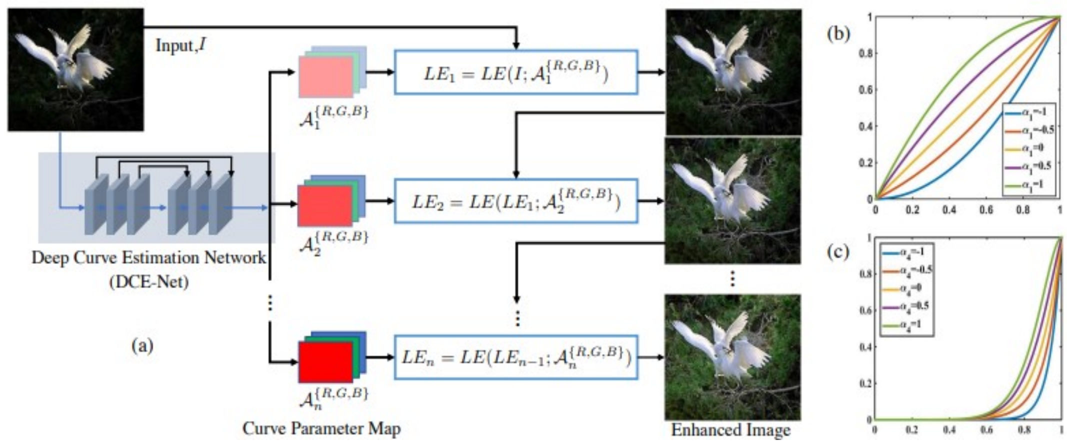

Fig.1

The MIT-Adobe Five dataset consists of 5,000 raw photos, each of which contains five retouching images created by skilled professionals. The LOL dataset of the paired low light / normal light photographs was obtained by varying the exposure length and ISO during image capture. In recent times, Wang et al. suggested an illumination map-estimated underexposed picture enhancement net work. Three specialists revised matched data before it was used to train this network. Picture light enhancement methods on the paired data are unworkable in many ways given the high cost of amassing sufficient amounts of paired data and the inclusion of false and unrealistic data when training the depth of models.

III. Methodology

The framework of the project is made to determine the optimal collection of Light-Enhancement curves (LE-curves) to use with an input picture. The framework then applies the curves repeatedly to map every pixel of the input RGB channels to produce the final improved image. The key components of this project, such as the LE-curve, DCE-Net, and non-reference loss functions, are filled in further information in the below details.

3.1. Curve of light-enhancement

To automatically transfer an unclear image to its improved counterpart, we strive to develop a curve whose own curve variables simply depend on the given image. The curve changes seen in picture editing software served as inspiration for that curve. Three objectives are in mind when such a curve is created: Each pixel value in the value-enhanced image should fall within the normalized range of [0,1] to prevent information loss due to overflow truncation. Additionally, this curve should be monotonous to preserve the differences (contrast) of the neighbouring pixels. For the gradient back propagation procedure, this curve's form should be as simple and differentiable as feasible. We create a quadratic curve to accomplish these three goals, which may be written as

$$LE(I(\mathbf{x}); \alpha) = I(\mathbf{x}) + \alpha I(\mathbf{x})(1 - I(\mathbf{x})), \quad (1)$$

We display the This project framework. A Deep Curve Estimation Network (DCE-Net) is made to determine the optimal Light Enhancement curves (LE-curves) to use with an input image. The framework then applies the curves repeatedly to map each RGB channel's pixels to create the final improved image. The next sections go into more detail about the crucial elements of This project, including the L E-curve, on-reference loss functions, and DCE-Net.

To automatically transfer a low-light image to its improved counterpart, we strive to develop a curve whose self-adaptive curve parameters simply depend on the input image. The curve changes seen in picture editing software served as inspiration that of curves. Three objectives are in mind when such a curve is created: Each pixel value in the improved image should fall within the normalized range of [0,1] to prevent information loss due to overflow truncation. This curve should also be monotone to maintain the contrast between adjacent pixels. For the gradient back propagation procedure, this curve's form should be as simple and differentiable as feasible.

Higher-order curve. Iteratively using the LE curve from Eq. enables more flexible modification to handle difficult low –light situations. Specifically,

$$LE_n(\mathbf{x}) = LE_{n-1}(\mathbf{x}) + \alpha_n LE_{n-1}(\mathbf{x})(1 - LE_{n-1}(\mathbf{x})), \quad (2)$$

Where ‘n’ is the iteration count, which determines the curvature. In this work, the total value of n is fixed at 8, which can satisfactorily handle the majority of scenarios. When n is 1, Eq. (2) may be reduced to Eq. (1). This depiction of a high-order curve with a different n has a stronger adjustment capacity.

Pixel-wise curve. An image in a more extended dynamic range can be adjusted by a higher-order curve. Since it is applied to every pixel, there is still a worldwide adjustment. Global mapping frequently over- or under-emphasizes local regions. To address this problem we create a pixel-wise parameter that modifies the multiple ranges by assigning the best-fitting curve to each part of the input picture. Hence, Eq. (2) may be expressed as follows:

$$LE_n(\mathbf{x}) = LE_{n-1}(\mathbf{x}) + \mathcal{A}_n(\mathbf{x}) LE_{n-1}(\mathbf{x})(1 - LE_{n-1}(\mathbf{x})), \quad (3)$$

Whereas is a parametric map with the same size as the image that was provided. As it is expected that pixels in a small region have the same intensity, the neighbouring pixels in the final output continue to keep their monotonic relations. The screen greater curves also accomplish these three objectives. We provide detail of the generated curve parameter maps for the three channels. The finest parameter maps for the different channels, which already have equal adjusting patterns but different values, demonstrate the relevance and variations between both the four systems of a lowlight image.

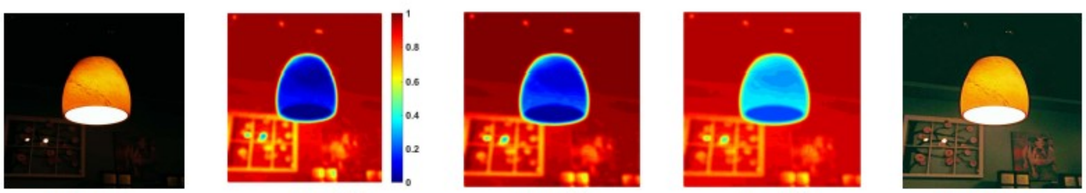

(a) Input (b) $\mathcal{A}_n^R$ (c) $\mathcal{A}_n^G$ (d) $\mathcal{A}_n^B$ (e) Result

Fig.2

3.2. DCE-Net. We propose that the greatest curve variable mappings for an input image be learned using a Deep Curve Estimation Network. (DCE-Net). A low-light vision serves as the DCE input, Net's and its outputs are a series of resolution curve variable maps to match higher-order curves. Seven symmetrical stacked convolutional make up the conventional CNN that we employ. 32 reversible neurons of size 33 and walk 1 are placed after the activation function in each layer. We eliminate the down sampling and group normalization settings that break pixel connections. The arrive-at-conclusion layer is backside by the Linear activation algorithm, which creates 24 variable maps 8times(n = 8).Three curved variable maps are required at each loop for the 3 colour channels. The supplementary data provides a detailed description of the DCE Net design. It is interesting to note that DCE-Net only has 79,416 practiced variables and 5.21G turns for value an input image with a size of 256 256 3. It is thus portable and appropriate for computing-constrained devices like cell phone devices.

*3.3. Non-reference loss functions***.** We offer some variation semi-losses that aid in negligible training in DCE-Net and give us the to find the value of improved pictures. The four losses described below are exact to instruct our DCE-Net. Topological integrity is lost. Incoherent spatial organization spa encourages spatial coherence of the enhanced image by maintaining the contrast among neighbouring areas in the actual picture and its increased form:

$$L_{spa} = \frac{1}{K}\sum_{i=1}^{K}\sum_{j\in\Omega(i)}(|(Y_i - Y_j)| - |(I_i - I_j)|)^2, \quad (4)$$

when K is the maximum number of nearby regions and I stands for the 4 regions that are equally placed on the zone (top, down, left, and right). In the enhanced rendition and input picture, respectively, Y and I stand in for the usual intensity value for the locality. Experimental results showed that the region zone had a 4 x 4 size. This loss is unaffected by changing area sizes.

(a) Input (b) Zero-DCE (c) w/o L_{spa} (d) w/o L_{exp} (e) w/o L_{col} (f) w/o $L_{tv_{\mathcal{A}}}$

Fig.3

Lack of exposure control. To manage exposure levels and prevent regions from being under or overexposed, we develop an effective preventive loss Leap. The difference between the average local intensity value and the region to the E amount of exposure is measured by the exposure control loss. We chose E as the Gary level in the RGB colour space to known norms [23,24]. Although we did not see a major performance change when we adjusted E between [0.4, 0.7], we set E at 0.6 in our tests. One way to express the loss Leap is as follows:

$$L_{exp} = \frac{1}{M}\sum_{k=1}^{M} |Y_k - E|, \tag{5}$$

where M is the number of 16 no overlapping local areas, and Y is the local region's average intensity value inside the augmented picture.

Lack of colour constancy. By using the Gary-World colour constancy theory [2], which asserts that colour in each sensor channel averages to Gary throughout the whole image, we constructed a colour constancy loss to correct any potential colour discrepancies in the image. Enhanced the picture and improve the links between the three changed channels. The colour consistency loss Local might be expressed as follows:

$$L_{col} = \sum_{\forall(p,q)\in\varepsilon}(J^p - J^q)^2, \varepsilon = \{(R,G),(R,B),(G,B)\} \tag{6}$$

where (p,q) designates some of the channels and Jpg stands for the p station's highest value in the improved image.

Lack of illumination smoothness. To keep relationships between related values monotonic, we take an additional step. Each curve parameter represents the uniform loss of light in A. The light smoothness loss Lava specifies the following:

$$L_{tv_{\mathcal{A}}} = \frac{1}{N}\sum_{n=1}^{N}\sum_{c\in\xi}(|\nabla_x \mathcal{A}_n^c| + \nabla_y \mathcal{A}_n^c|)^2, \xi = \{R,G,B\} \tag{7}$$

where x and y stand in for the horizontal and vertical gradient processes, respectively, and N is one of the iterations.

Lose overall. The overall loss is stated as follows:

$$L_{total} = L_{spa} + L_{exp} + W_{col}L_{col} + W_{tv_{\mathcal{A}}}L_{tv_{\mathcal{A}}}, \tag{8}$$

where Wool and WV represent the losses' weights.

IV. BREAK THROUGH

***Details of implementation*.** CNN-based models frequently employ self-captured paired data for network training [5, 17, 28, 30, 32, 33], while GAN-based models deliberately choose unpaired data [6, 11, 12, 16, 35]. To effectively utilize the potential of broad dynamic range correction, we include both low-light and overexposed photographs in our training collection. We employ 360 multi-exposure patterns from Part 1 of the SICE data to train the proposed DCE-Net [4]. Enlighten GAN [12] also uses the dataset as trained data. We randomly split 3,022 images with varying exposure levels into two groups for the Part 1 subgroup [4]. The practice images are scaled down to 512 by 512 pixels. Using an NVIDIA 2080Ti GPU, Porch is used to test our system. The set group number is 8. The initial setting of each layer's filter weights is a Gaussian function with a typical zero mean and 0.02 standard deviation. Bias starts at a fixed value. We use the ADAM method with present parameters and a fixed learning rate of 1e4 for our network optimization. The weights Wool and WV are fixed at 0.5 and 20, respectively, to balance the size of losses.

4.1. Ablation study

To show the efficacy of each This project component, we conduct several ablation experiments as follows. The supplementary information contains additional qualitative and quantitative analyses.

***Each loss' contribution*.** In fig.3 we display the outcomes of Zeroed trained using different combos of losses. The outcome with no lack of spatial integrity Laps has less contrast than the complete result, for instance in the cloud storage areas. This demonstrates the value of Laps in maintaining the distinction between nearby areas in the original and improved images. the exposure control loss is eliminated L expr is unable to restore the dim area. When the colour consistency loss Local is ignored, severe colour shadows appear. When applying curve mapping, this version skips the relationships between the three channels. Lastly, addressing the lack of light smoothness Latvia interferes with the relationships between nearby areas, producing glaring artefact's.

Effect of parameter settings. We evaluate the effects of This project's factors, which include the DCE-Net's depth and diameter also to the quantity repetitions. Fig. 5 illustrates in graphic form. This project3328 can already yield acceptable results in Fig. 5(b) with just three convolutional layers, demonstrating the potency of zero-reference learning. With appropriate contrast and natural exposure, the This project7-32-8 and This project7-32-16 create the most aesthetically pleasing outcomes. On This project732-1, a clear decline in efficiency is seen when the one of repetitions is reduced to 1, as in Fig. 5.This is due to the curve's restricted ability to be adjusted after a single repetition. This implies that our approach needs higher-order shapes. Given its favourable trade-off between economy and restoration performance, we decided to use This project7-32-8 as the ultimate model.

Training data impacts. To investigate the features of training data, we give the project on a variety of datasets. Just 900 of the 2,422 pictures in the quality training dataset (This project Low) were taken in low light, leaving 9,000 low-light images unidentified. 3) 4800 multiple photographs from the SICE data [4]'s data-augmented collaboration of P1 and P2 subsets; pictures from the dark dataset [37] (Zero DCE Huge L) (This project Large LH). Although utilizing more low-light photos, as illustrated in Fig. 6(c) and (d), This project tends to over-enhance the well-lit parts (such as the face) after eliminating the overexposed training data (i.e., This project Large). These results support the rationale and necessity of training our network with multi-exposure training data. Moreover, as in Fig. 6, the advantage of additional multi-exposure training data (i.e., This project Big LH) allows the Zero DCE to successfully recover the dark regions (e). Although more training data could enhance the visual performance of our technique, we use comparable volumes of training data to other deep learning-based methods to compare them equitably.

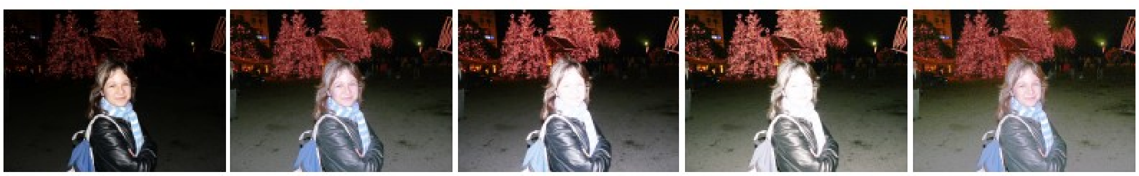

(a) Input (b) Zero-DCE (c) Zero-DCE$_{Low}$ (d) Zero-DCE$_{LargeL}$ (e) Zero-DCE$_{LargeLH}$

Fig.4

4.2. Benchmark assessments. We compare This project with several state-of-the-art methods, such as two CNN-based methods (retime Net [32], Li et al. [19]), three conventional methods (LIME [9], SRIE [8], and Li et al. Wang et al. [28]), and one GAN-based method (Enlighten GAN [12]). It is important to use publicly available source codes with recommended parameters to replicate the results. We undertake qualitative and quantitative research using standard picture sets from earlier publications, including NPE [29], LIME [9], MEF [22], DICM [14], and VV. The 229 multi-exposure sequences and corresponding reference pictures from the Part2 subset of the SICE dataset are also used to statistically test our method [4]. We only examine the low-light photos from the Part2 subset [4] to ensure a fair comparison, as baseline techniques are insufficient for handling overexposed images. We deliberately choose the first three (or four) low-light photos from a multi-exposure sequence if there are seven (or nine) shots total, and we resize each image to 12009003. 767 pairs of low/normal light photographs are ultimately collected. Because retime Net [32] and Enlighten GAN [12] both use part of the pictures from this dataset in their training datasets, the low/normal light picture dataset stated in [37] is ignored. The most current paired training and testing dataset developed in [28] is not given to the wider public, so keep that in mind. We did not utilize the MIT-Adobe Five dataset [3] since it is not specifically designed to enhance underexposed photos.

4.2.1 Comparing the visual and perceptual

In common low-light photographs, we present visual comparisons. For challenging backlit areas (like the face), this project creates natural exposure and clear details. Retime Net [32] generates overexposed artefact's. In the second example, which depicts an interior scene, our method simultaneously enhances the gloomy parts while preserving the original image's colon. The result is aesthetically pleasing due to the absence of overt noise and colour casts. Contrastingly, [19] smooth the features, but other baselines amplify noise and even cause colour departure. We undertake user research to qualify the subjective image quality of various methodologies. We process images in low images. using a variety of photo set strategies (NPE, LIME, MEF, DICM, and VV). We display each enhanced result on a screen beside the original image as a reference. A total of 15 human participants will independently rate the enhanced image's visual quality.

Ratings for visual quality range from 1 to 5. from poorest to highest quality. The average opinion ratings for each set of photographs are shown in Table 1. This project earns the highest average User Study (US) score for a total of 202 testing images from the aforementioned image collections, as shown in Table 1. The MEF, DICM, and VV sets are where the respondents prefer our findings the most. In addition to the US score, we also utilize a non-reference perception index (PI) [1, 21, 25] to rate the visual quality. The PI metric's original goal was to rate the perceived quality of super-resolution photographs. The effectiveness of other image restoration tasks, such as picture debasing, has also been assessed using this method [26]. A lower PI number indicates better perceptual acuity. The PI values are also summarised in Table 1. Similar to what the user survey revealed, the recommended This project outperforms other competing strategies in terms of average PI values.

Better human subjective visual quality is indicated by the US score. The winning outcome for each case is shown in red, while the runner-up is shown in blue.

4.2.2 Comparative measurements

We statistically assess the performance of several approaches on the Part2 subset using the Peak Signal-to-Noise Ratio (PSNR, dB), Structural Similarity (SSIM) [31], and Mean Absolute Error (MAE) metrics [4]. The proposed This project in Table 2 still achieves the best outcomes in all circumstances despite not utilizing any paired or unpaired training data. Due to the basic curve mapping form and thin network design, this project is also numerically efficient. Table 3 shows the average runtime for several approaches for 32 images with a resolution of 1200 by 900 pixels. With conventional methods, just CPU version codes are given.

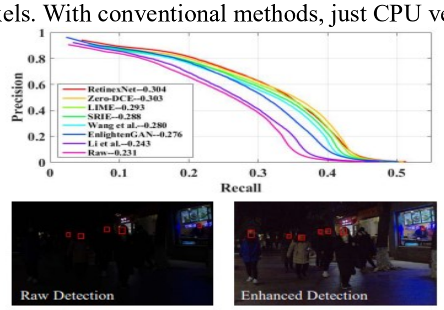

Fig.5

V.KIVY FRAMEWORK

For the motive of creating multi touch apps for mobile devices and other platforms, Ivy is an open-sourced and free Python-based scripting framework. It is published under the condition of MIT-License and works with Android, is, Linux, macros, and Windows. The Ivy group has created various libraries that may be used on all platforms, including Python for Android and ions, and key, which is the primary framework. The Python Software developers awarded Ivy a grant of $5000 in 2012 for the conversion to Python 3.3. The Raspberry Pi, which was sponsored by Bounty source, is also supported by key.

VI. BULLDOZER TOOL

A program called Bulldozer makes it simple to bundle mobile applications. The whole build process is automated, and requirements like python-for-android, and Android are downloaded. Bulldozer maintains a file called Bulldozer. Spec in your application directory that lists the specifications and preferences for your program, including its title, icon, modules, and other details. It will produce a package for Android and iOS, and other platforms using the specification file.

VII.CONCLUSION

We proposed this paper to get good images using mobile applications. That app was fully developed using python. For the improvement of low-light images, we suggested a complete network. With no reference photos, this trained data from beginning to end. To do this, a collection of differentiable no reference losses are created for the low-light picture improvement job and is designed as an image-specific curve estimate issue. Tests show how effective our technology is compared to remaining light augmentation techniques. In our upcoming work, we'll strive to use semantic information to answer challenging problems and take noise into account. The main thing of this paper is that implemented into a python application. That was created by the KIVY and the application was developed using the Bulldozer tool.

REFERENCES

[1] Tamer Michaela and Yoshi Belau. A trade-off between perceptual distortion. 2018. In CVPR.GershonBuchsbaum.

[2] Example of the spatial processor for the perception of object colour. 310(1):1-26 in J. Franklin Institute, 1980.

[3] Freda 'Durand, Eric Chan, Sylvain Paris, and Vladimir Bychkovsky. With the data of input and output image pairings, one may learn photographic global tone correction. 2011. In CVPR.

[4] Lei Zhang, Shu hang GU, and Jeanie Cain. From multiple images, learning a deep one-image contrast is cleaner. 2018;27(4):2049–2026;IEEEcommunicate on Image Processing.

[5] Kolton- Ladle, Jian-Xu, Chen-Chen, and Qi Feng-Chen. mastering the art of night vision. 2018. In CVPR.

[6] Yachting Wang, Mansion Kao, Hushing Chen, and Yungyu Chuang. Minute photo enhancer: GANS-based image improvement from images using learning. 2018. In CVPR.

[7] C.Nagarajan and M.Madheswaran - 'Stability Analysis of Series Parallel Resonant Converter with Fuzzy Logic Controller Using State Space Techniques'- *Taylor & Francis, Electric Power Components and Systems*, Vol.39 (8), pp.780-793, May 2011.
[8] Nagarajan and M.Madheswaran - 'Experimental Study and steady state stability analysis of CLL-T Series Parallel Resonant Converter with Fuzzy controller using State Space Analysis'- *Iranian Journal of Electrical & Electronic Engineering*, Vol.8 (3), pp.259-267, September 2012.
[9]
[10] Jean-Marc Chaser, Philippe-Bolton, and Dina Cultic. Histogram precision specifications. (2005) IEEE communicate on Image enhance, 15(5), pp. 1143–1152.
[11] Deli-Zeng, Xiao-Ping-Zhang, Yue-Huang, Guiyang-Fu, and Xanga-Ding. a weighted difference model for estimating light and reflectance simultaneously. In CVPR, 2016.
[12] Hailing-Ling, Yu-Li, and Xiaojie-Guo. Lime: Illumination map estimate for low-light picture enhancement. 2017; 26(2):982-993; IEEE communication on Image enhance.
[13] Nicholas-Sai-Pik-Kong and Heidi-Ibrahim. Dynamic graphics equal brightness preservation for improving image contrast. The 2007 edition of IEEE communication on customer Electronics, 53(4), pages 1752–1758.
[14] Andrey-Ignite, Luc Van Goal, Raju Timofte, Nicolai Kobyshev, and Kenneth Vanhoey. Wespe: A poorly regulated digital camera photo enhancement tool. 2018 in CVPRW
[15] **C.Nagarajan** and M.Madheswaran - 'Experimental verification and stability state space analysis of CLL-T Series Parallel Resonant Converter' - ***Journal of ELECTRICAL ENGINEERING,*** Vol.63 (6), pp.365-372, Dec.2012.
[16] **C.Nagarajan** and M.Madheswaran - 'Performance Analysis of LCL-T Resonant Converter with Fuzzy/PID Using State Space Analysis'- ***Springer, Electrical Engineering***, Vol.93 (3), pp.167-178, September 2011**.**
[17] .
[18] Pan-Zhou, Jianchao-Yang, Xinyu-Gong, Ding-Liu, Yu-Cheng, Chen-Fang, Xiaohui-Shen, and Zhangyang-Wang. EnlightenGAN: Enhancing the deep light without a partner's supervision. 2019 in CVPR.
[19] Edwin-H-Land, p. 13. The colour vision retina hypothesis. 108–128, Scientific American, 237(6), 1977.
[20] Chula-woo-Lee, Chang-Su Kim, and Chula Lee. improvement of contrast via ordered variety representation. 2012, ICIP.
[21] Chang-Su Kim, Charlwood Lee, and Chula Lee. Enhancement of contrast using layered differences in 2D histograms. 2013's IEEE communication on Image enhance, 22(12), pages 5372–5384.
[22] Chunnel-Guo,Jichang-Guo, and Chongjin-Li. Using weakly classificationcolor transfer, underwater picture colour correction. 2018 IEEE Signal Processing Letters, 25(3), pp. 323–327.
[23] **C. Nagarajan, G.Neelakrishnan, R. Janine, Maithili, G. Ramya "**Investigation on Fault Analysis for Power Transformers Using Adaptive Differential Relay" Asian Journal of Electrical Science, Vol.11 No.1, pp: 1-8, 2022.

[24] G.Neelakrishnan, K.Anandhakumar, A.Prathap, S.Prakash "Performance Estimation of cascaded h-bridge MLI for HEV using SVPWM" Surah Pun Journal for Multidisciplinary Research, 2021, Volume 11, Issue 4, pp:750-756
[25] of T-Source Inverter fed with Solar Cell" Surah Pun Journal for Multidisciplinary G.Neelakrishnan, S.N.Pruthika, P.T.Shalini, S.Soniya, "Performance Investigation Research, 2021, Volume 11, Issue 4, pp:744-749
[26] G.Neelakrishnan, P.Iraianbu, T.Abishek, G.Rajesh, S.Vignesh, "IOT Based Monitoring in Agricultural" International Journal of Innovative Research in Science, Engineering and Technology, March 2020, Volume 9, Issue 3, pp:814-819
[27] G.Neelakrishnan, R.S.Jeevitha, P.Srinisha, S.Kowsalya, S.Dhivya, "Smart Gas Level Monitoring, Booking and Gas Leakage Detector over IOT" International Journal of Innovative Research in Science, Engineering and Technology, March 2020, Volume 9, Issue 3, pp: 825-836
[28] Yanwei Pang, FatihPorikli, Chongyi Li, and Jichang Guo. The conversion neural network process called Lightennetimproves images with poor lighting. 2018; 104:15–22, Pattern Recognition Letters.
[29] Jian-Li, Feiyuen-Huang, Jilin-Li, Chongjin Wang, Yabba-Wang, Changing-Wang, Ying-Tai, Jian Jun-Qian, Jian-Yang. Dual shot face detector (DSFD). 2019 in CVPR.
[30] Madding-Li, Jialing-Liu, Zinging-Guo, Wenhan-Yang, and Xiaoyan-Sun. Using a reliable retained model, structure-revealing low-light picture enhancement. 2018; 27(6):2828–2841 in IEEE communication on Image Enhancement.